ISSN: 2054-7412 Volume 2, Issue 1 - February 2014

# AIVP

## ADVANCES IN IMAGE AND VIDEO PROCESSING

Society for Science and Education
United Kingdom

# TABLE OF CONTENTS

## EDITORIAL ADVISORY BOARD

## DISCLAIMER

**All the contributions are published in good faith and intentions to promote and encourage research activities around the globe. The contributions are property of their respective authors/owners and the journal is not responsible for any content that hurts someone's views or feelings etc.**

AIVP ADVANCES IN IMAGE AND VIDEO PROCESSING
SOCIETY FOR SCIENCE AND EDUCATION UNITED KINGDOM
VOLUME 2, ISSUE 1
ISSN: 2054 - 7412

# Quality Measurement for Reconstructed RGB Image via Noisy Environments

**Muthana H. Hamd, Rabab Abd Rassol**
*Computer/ Faculty of Engineering, Al Mustansirya University, Baghdad, Iraq*
muth700@yahoo.com; rabab_rassol@yahoo.com

**ABSTRACT**

Image compression and decompression process could be quite affected by noisy environment during transmitting/receiving medium. This paper develops a procedure which finds the effect of noisy environments on the reconstructed RGB images. The image has been degraded by three kinds of noises then; noisy image planes are transformed into new domain of four bands by applying the first level 2D DWT. The inverse 2D DWT is applied on the noisy RGB planes to reconstruct; concatenate; and restore the original transmitted image. The quality of re-stored images is measured by applying SNR/PSNR with respect to the noise variances. The SNR/PSNR dB curves are used for comparing different noisy environment effects on the quality of reconstructed RGB images. The paper provides basic procedure for calculating scale factors used for reconstructing images directly in SNR/PSNR units. The SNR/PSNR dB curves for Gray images satisfied better result than RGB for all testing conditions, while speckle noise was relatively the most stable degrading noise that had maximum dB values over wide noise variance. Salt & pepper noise had the worst dB curves among Gaussian and speckle. The intersection points of the dB curves at 0.5 density noise is discussed and concluded to find out the SNR/PSNR behavior at this degradation value.

*Keywords:* DWT, IDWT, RGB, SNR, PSNR, noise

## 1.INTRODUCTION

The RGB color system represents the most commonly used in computer fields, although there are an infinite number of color spaces. Most of those color systems are derived from the RGB color space by applying linear transforming function of R, G, and B. Image compression is a one area that Discrete Wavelet Transform (DWT) has proven its applicability in reconstruct the compressed image efficiently, even better than Discrete Cosine Transform (DCT) method. To compress the RGB image, it is recommended to apply one of compression algorithms; likes DCT or DWT. The three RGB planes should be first separated and processed as a 2D gray image. The compressed image can be transmitted quicker and then decompressed faster by the receiver [ 1,2 ]. A compression algorithm object is to remove the redundancy in image data by exploiting

**DOI**: 10.14738/aivp.21.35
**Publication Date:**10th February 2014
**URL**: http://dx.doi.org/10.14738/aivp.21.35

these redundancies in a way that makes the reconstruction is possible. The entropy ($H_e$) finds the minimum limit representation of grey bit that value should not be exceeded during compression. For example, an image has M grey levels and P(k) probability for level k, the entropy formula is [ 3,4]:

$$H_e = -\sum_{i=1}^{M} P(k) log_2 \ [P(k)] \qquad (1)$$

The compressed gray level would be encoded within this boundary: $H_e \leq L_{comp} \leq L_{(fixed)}$

Where:

$L_{(fixed)}$ : $2^n$ fixed length code

$L_{comp}$ : The new compressed code

This paper develops a proposed testing system that applies an evaluation procedure to measure the reconstructed noisy RGB image quality using Signal to Noise Ratio (SNR) and Peak Signal to Noise Ratio (PSNR). The transformed RGB image was injected by wide scale of noise variance of noisy environments, so quality measurement of the reconstructed and de-noised RGB image is calculated to study the decibel curves behaviour with respect to the noise variances. The PSNR is the most commonly used as quality measurement of the reconstructed lossy compressed images. It is the ratio between the max ***possible*** signal power to the power of the corrupted noise. It is derived by setting the mean squared error (MSE) in relation to the maximum possible value of the luminance (for a typical 8-bit value this is -1 = 255) as follows [5, 6, 7]:

$$PSNR = 20. log_{10} \left[\frac{255}{\sqrt{MSE}}\right] \qquad (2)$$

Where (MSE) is the mean squared error between the origin and destination image,

$$MSE = \frac{\sum_i^M \sum_j^N [\, f(\,i,j\,) - g(i,j)\,]^2}{M.N} \qquad (3)$$

The SNR is defined as the power ratio between the original signal and the unwanted background noise:

$$SNR = 10. log_{10} \left[\frac{\sum_i^M \sum_j^N [\, f(\,i,j\,)\,]^2}{\sum_i^M \sum_j^N [\, f(\,i,j\,) - g(i,j)\,]^2}\right] \qquad (4)$$

Where:

$f(\,i,j\,)$: *is the original image*

$g(i,j)$ : is the destination or degraded image

## 2.EVALUATION PROCEDURE

The general block diagram of the proposed testing system that runs the evaluating procedure as stages is explained in figure 1. Mainly it includes:

- Noise(s) injection and RGB planes separated
- Analysis / synthesis of noisy RGB planes
- De-noising and image planes concatenated
- Quality measurement using SNR/PSNR

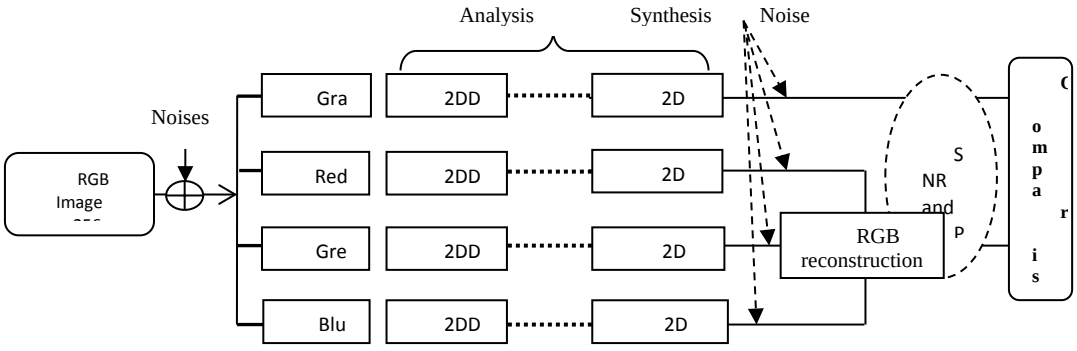


Figure 1 General block diagram of evaluation system.

### 2.1 Noise(s) injection and RGB planes separated

The proposed noisy environment contains three kinds of noises. These noises are injected to the RGB image sequentially (separately) or simultaneously (mixed). These noises are:

- Salt and pepper: also called shot, impulse, or binary noise and it is happened because of sharp, sudden, and random change in the image signal.
- Gaussian noise: also called additive noise, it is the idealized form of white noise; it is caused by random fluctuations in the image signal. If I represents the image signal, and $N_g$ is the Gaussian noise, then:

$$I' = I + N_g \qquad (5)$$

- To remove the degradation of this kind of noise, a mean filter is applied as explained in equation (6).

$$I' = \frac{1}{100}\sum_{i=1}^{100}(I + N_g) \qquad (6)$$

- Speckle noise: also called multiplicative noise; it is the major problem in some radar and medical applications. Median or mean filter are the more suitable filters for denoising image that degraded with this kind of disturbance.

$$I' = I(1 + N_{sk}) \qquad (7)$$

The degradation procedure is implemented using one of two methods:

**First method:** Noises are injected in the original RGB image then SNR/PSNR evaluation is calculated for each red, green, and blue matrix separately

**Second method:** Noises are injected on each red, green, and blue plane separately then SNR/PSNR is calculated for their Gray and RGB equivalent. The two methods are qualified and compared using the PSNR dB curves in figures 2 and 3. The decibel curves are very similar and relatively keep the same curve shape over wide variant noise values, except the Gray image of figure 2 which has maximum dB values comparing with other curves. So, decision is taken to consider the first method regarding noise injection procedure. These noises are injected using two modes: separately/sequentially or simultaneously/mixed to meet all probabilities of testing condition.

## 2.2 Analysis/Synthesis of noisy RGB planes

The DWT analysis is used to divide the information of image into approximation and detail subsignals. The approximation band represents the general shape of pixel values, while the other bands describe the horizontal, vertical, and diagonal details inside image. A simple formula is estimated from Wavelet transformation is:

$$\text{Number of Bands} = (\text{No. of levels} \times 3) + 1 \qquad (8)$$

The degraded RGB image is separated into three corresponding planes (red, green, and blue) as well as its equivalent noisy gray one. The next step is to apply the 2D DWT on the four noisy gray images. That means, the total number of transformed noisy images would be:

$$4_{(no.of\ noisy\ images)} \times 4_{(no.of\ bands)} = 16_{(4\ approx.band\ +\ 12\ detail\ bands)}.$$

Those bands are currently ready for compressing and re-constructing. The current stage is completed by finding the IDWT for those $16_{(128\times128))}$ bands, which means the four noisy images are composed again, they are; $red_{(256\times256)}$, $green_{(256\times256)}$, $blue_{(256\times256)}$, $gray_{(256\times256)}$

## 2.3 De-noising, concatenated, and quality measurement

This stage runs three processes, first one is to remove or decrease the amount of noise(s) in the reconstructed images using suitable filter, secondly is to concatenate and restore the original Gray and RGB image. The third process is to qualify the resulted images to find and discuss the factor which relates between the amount of injected noise(s) and the accepted SNR/PSNR dB unit. The noise scale is 23 values ranging from 0.01 to 1. Figures 4 and 5 represent the PSNR/SNR dB curves for mixed noise injection mode. The SNR/PSNR of" peppers.png" image for sequential noise injection regarding Gray and RGB images are explained in figure 6, 7, 8, and 9 respectively.

## 3. RESULT AND DISCUSSIONS

**Degradation Procedure:** figure 2 and 3 represent the results of the two degradation procedures. Procedure one degrades the RGB image then separates the individual planes while, the 2nd procedure separates the individual planes before making the degradation. The PSNR dB curves for two procedures are so closed except the gray image of procedure one which is satisfied max. PSNR (28.13 dB) comparing with (24.77 dB) for gray image in procedure two. So, the proposed evaluation procedure would consider the 1st procedure in the degradation method.

**PSNR/SNR Qualification:** figure 4 is the PSNR for mixed noises regarding Gray and RGB images. The max. PSNR value (29.91 dB) is satisfied with Gray image, while (26.87 dB) was the value of RGB image. The max. SNR value is satisfied with Gray image (21.24 dB), while (18.89 dB) was the max. value for RGB image as shown in figure 5. Figure 6 and 7 represent the SNR/PSNR qualification curves for Gray image. The maximum SNR/PSNR values are satisfied with speckle noise (25.32 dB) and (31.21 dB) respectively, while the Gaussian noise was the min. one with (20.12 dB) and (28.78 dB) respectively for noise density 10%. The reconstructed RGB images are qualified in figure 8 and 9. The speckle noise has max SNR/PSNR values with (24.82 dB) and (34.04 dB), while Gaussian noise has the min. SNR/PSNR value with (20.46 dB) and (28.40 dB) respectively.

**Crossing Values:** the decibel curves for Gaussian and Salt& pepper noise have a noticeable feature that they always crossing when the noise density is approximately 0.5. This means, the two noises have the same effectiveness at this value, so one of them could be substituted by another one. Example of these features are tabulated in table 1.

Table 1 Matching features for sequential noise injection with density equals 50%

| SNR Qualification (dB) | | | | PSNR Qualification (dB) | | | |
|---|---|---|---|---|---|---|---|
| Gray | | RGB | | Gray | | RGB | |
| *gaussian* | *salt* | *gaussian* | *salt* | *gaussian* | *salt* | *gaussian* | *salt* |
| 6.22 | 6.26 | 6.18 | 6.09 | 14.87 | 14.94 | 14.14 | 14.09 |

## 4. CONCLUSION

The evaluation procedures is proposed and implemented as quality measurement using SNR/PSNR. The RGB image is supposed to be transmitting via multi noisy environments so it is degraded with three kinds of noises. Then, the degraded RGB image is separated and transformed into 16 subbands using 2D DWT. The degraded and transformed sub-images are reconstructed by applying the inverse DWT. The RGB planes are re-concatenated again to measure and evaluate the SNR/PSNR for wide noise variance. At 0.5 density noise, the decibel

curves of Gaussian and salt& pepper noise are approximately same; also the Gray dBs and RGB dBs are approximately same. Also, the SNR/PSNR curves satisfied maximum dB values when the degradation is speckle noise, and minimum dB values are obtained from salt& pepper noise degradation. In SNR/PSNR units, the image is still usable when it's degraded with ≤ 0.5 mixed noises.

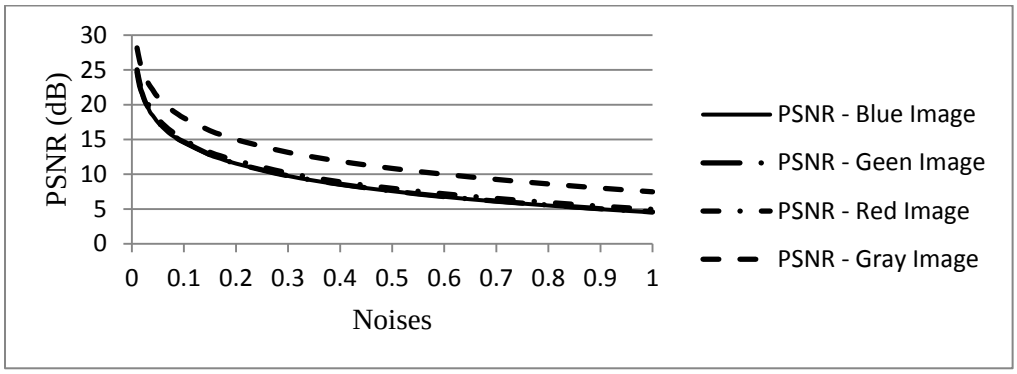


Figure 2. Quality mesurment using method 1 degradation

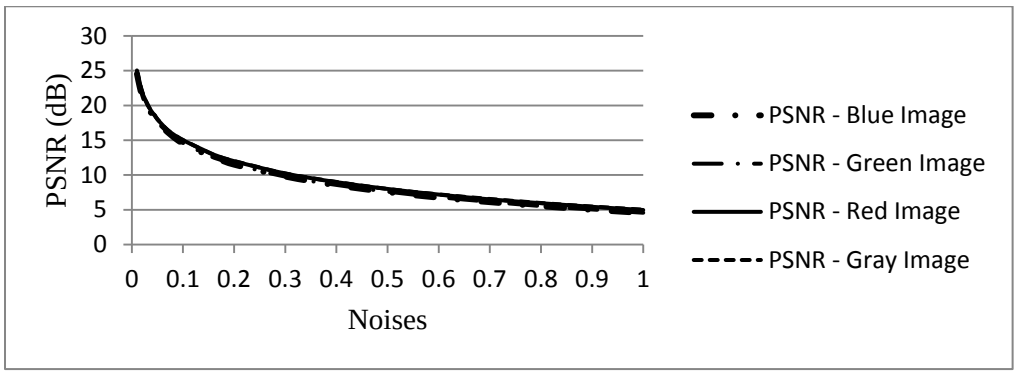


Figure 3. Quality mesurment using method 2 degradation

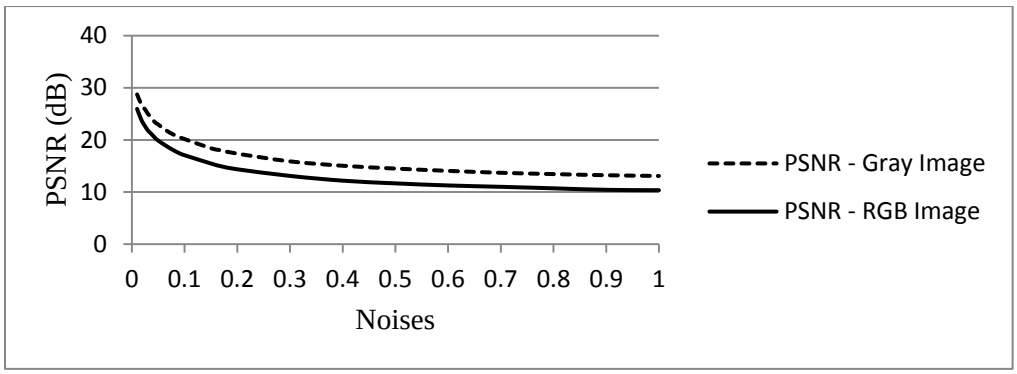


Figure 4 PSNR qualification for mixed degradation

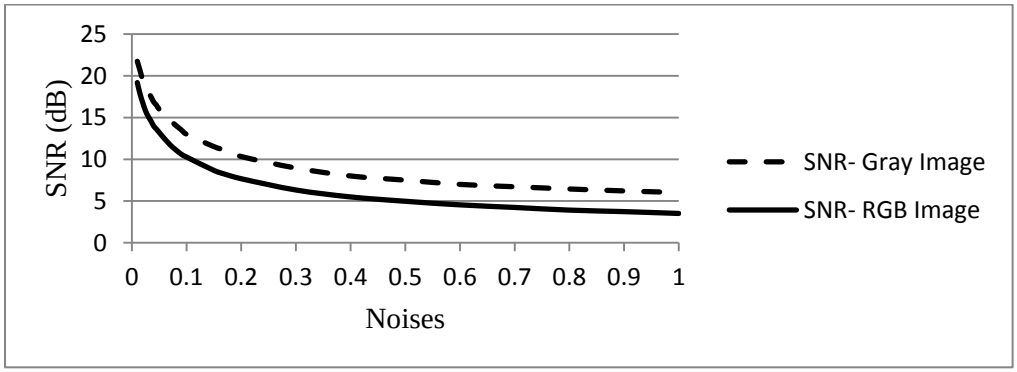


Figure 5. SNR qualification for mixed degradation

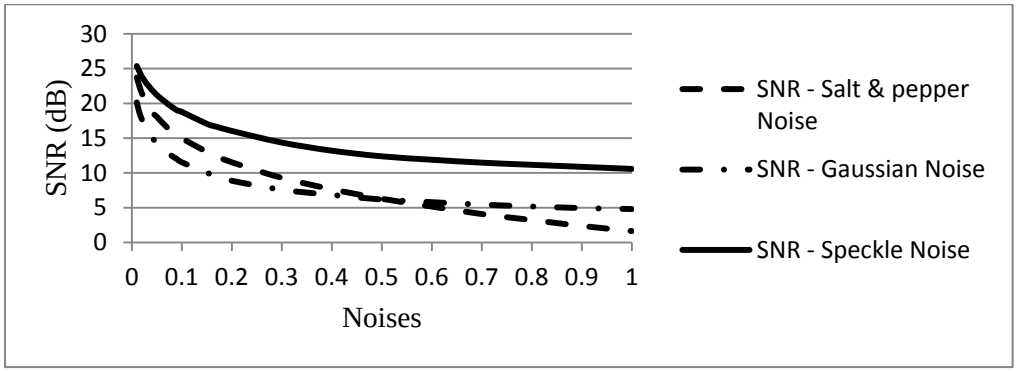


Figure 6. SNR qualification for sequential injection of Gray image

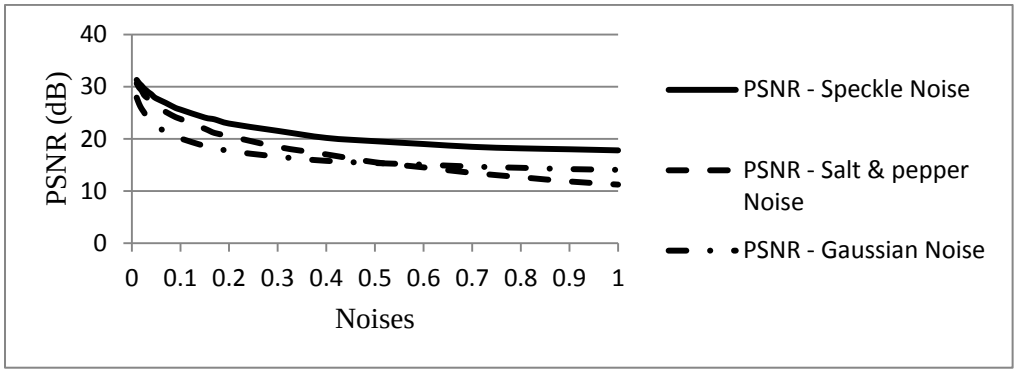


Figure 7. PSNR qualification for sequential injection of Gray image

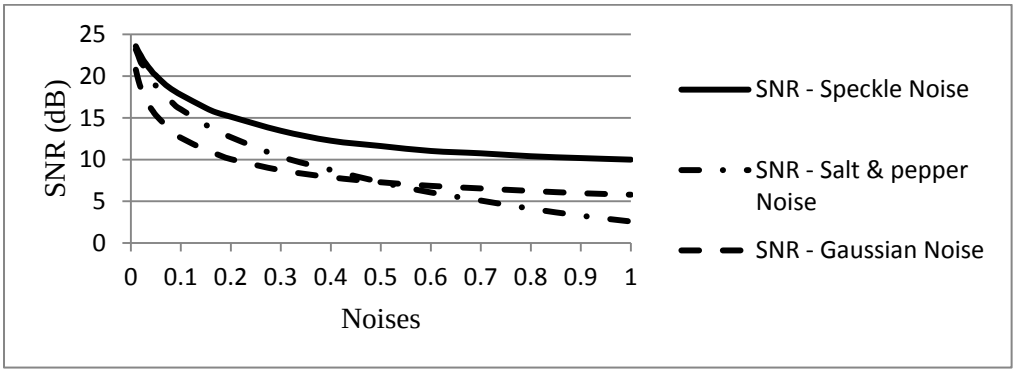


Figure 8. SNR qualification for sequential injection of RGB image

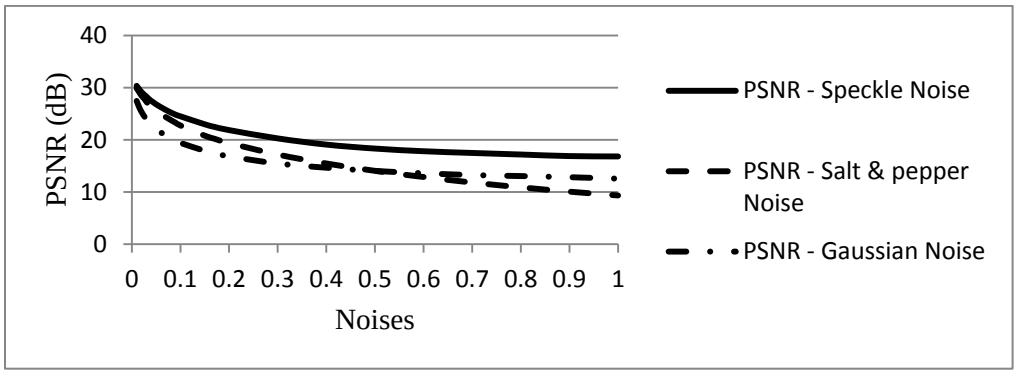


**Figure 9. PSNR qualification for sequential injection of RGB image**

## REFERENCES

[1]. K. H. Talukder and K. Harada, "Haar Wavelet Based Approach for Image Compression and Quality Assessment of Compressed Image", IAENG International Journal of Applied Mathematics, 36-1, IJAM_36_1_9, (2007).

[2]. M. Saraswat , A. K. Wadhwani and M. Dubey, "Compression of Breast Cancer Images by Principal Component Analysis", International journal of Advanced Biological and Biomedical Research, 1, 767-776, (2013).

[3]. J. S. Walker. Wavelet-based Image Compression (2nd Edition), University of Wisconsin, Eau Claire (1999).

[4]. S.S.Palewar and Ranjana Shende, "Watermarking Robustness Evaluation Using Enhanced Performance Metrics.", International Journal of Engineering Research & Technology (IJERT), 2, 2278-0181, (2013).

[5]. N. D.Venkata, T. D. Kite, B. L. Evans, and A. C. Bovik, "Image Quality Assessment Based on a Degradation Model", IEEE Trans. Image Proc. 9, 636-650, (2000).

[6]. Sungkwang Mun and J. E. Fowler, "BLOCK COMPRESSED SENSING OF IMAGES USING DIRECTIONAL TRANSFORMS", International Conference on Image Processing, Cairo, Egypt, 3021-3024, (2009).

[7]. Yusra A. Y. Al-Najjar and Der Chen Soong, "Comparison of Image Quality Assessment: PSNR, HVS, SSIM, UIQI", International Journal of Scientific & Engineering Research, 3, 8, 2229-5518, (2012).

[8]. A. Saffor and Abdul Rahman Ramli, "A COMPARATIVE STUDY OF IMAGE COMPRESSION BETWEEN JPEG AND WAVELET", Malaysian Journal of Computer Science, 14, 1, 39-45, (2001).

[9]. N. Salamati and Z. Sadeghipoor, "Compression of Multispectral Images: Color (RGB) plus Near-Infrared (NIR)", (2011).

[10]. N. Dey, A. B. Roy, and S. Dey, "A Novel Approach of Color Image Hiding using RGB Color planes and DWT", International Journal of Computer Applications, 36, 5, 0975 – 8887, (2011).

AIVP ADVANCES IN IMAGE AND VIDEO PROCESSING
SOCIETY FOR SCIENCE AND EDUCATION UNITED KINGDOM
VOLUME 2, ISSUE 1
ISSN: 2054 - 7412

# Laplacian Pyramid based Hierarchical Image Inpainting

**[1]S. Padmavathi, [2]K. P. Soman**
*[1] Department of Information Technology*
*[2]Head of CEN department*
*Amrita School of Engineering, Coimbatore, India.*
[1]s_padmavathi@cb.amrita.edu,[2] kp_soman@amrita.edu

**ABSTRACT**

There are many real world scenarios where a portion of the image is damaged or lost. Restoring such an image without prior knowledge or a reference image is a difficult task. Image inpainting is a method that focuses on reconstructing the damaged or missing portion of images based on the information available from undamaged areas of the same image. The existing methods fill the missing area from the boundary. Their performance varies while reconstructing the structure and texture present in the image and majorly fails for larger inpainting area. This paper attempts to segregate the structure and texture using Laplacian Pyramid and inpaint them separately using a top down approach. The images are inpainted from the lowest spatial resolution using Exemplar based image synthesis. The results are updated before moving to the higher resolution levels. This multi resolution process ensures the coarser details being filled before the finer details. The structure propagation is better since it is handled separately. The top down approach alleviates the traditional boundary based filling and breaks the single large sized inpainting region into many smaller sized ones as we move down the pyramid. Different types of images have been experimented and the results are summarized.

**Keywords**: Hierarchical Digital Image Inpainting, Laplacian Pyramid, Exemplar based Inpainting, Multiresolution Inpainting

## 1.INTRODUCTION

In olden days, artists reconstructed the damaged paintings by propagating the colors in the boundary of damaged parts. This process was known as inpainting. Bertalmio et al [10] used a digital version of the technique to restore cracks in photos and to remove inscribed texts on digital images and called it as Digital image Inpainting. In general, the term image inpainting refers to the synthesis of the damaged, missing or hidden portion of the image in a visually plausible way. Inpainting is used in a primitive form in certain image editing software. They expect the user to specify the area to be inpainted and also specify the sample that has to be put in its place. Digital image inpainting requires the user to specify the area to be inpainted,

**DOI**: 10.14738/aivp.21.46
**Publication Date:**10th February 2014
**URL**: http://dx.doi.org/10.14738/aivp.21.46

but fills it automatically using the information available in the surrounding area of the same image. The inpainting problem is also addressed under disocclusion, object removal etc. The applications of inpainting includes removal of cracks from a damaged photograph, retrieving the damaged portions of digital paintings, removing unwanted texts and objects in a scenic photograph, removing the obstacles and retrieving the hidden background, removing the objects to create special effect etc.

The propagation of the information into the inpainted area determines the success of the algorithm. The geometric and the photometric propagation which is generally called as structure and texture propagation poses a major challenge to inpainting algorithms. Partial differential equations based inpainting algorithms perform well for smaller inpainting areas. Texture synthesis based methods work well for larger areas but fail in geometric propagation. Exemplar based methods which is a kind of texture synthesis technique performs reasonably well for larger areas but fails in structure propagation at a larger scale. The technique presented in this paper is inspired by the response of Human visual system in viewing a photograph from various distances. When viewed from a larger distance only the coarser information in the image could be viewed. As the distance reduces the finer details could be seen. Hence filling in the coarser information and then the finer information will result in better reconstruction. The Phenomenon is best imitated by the image pyramid discussed by Burt and Adelson in [1], with the image viewed from farthest distance at the top of the pyramid and the image viewed at the closest distance at the bottom of the pyramid. In general the actual image forms the bottom and its smoothened version, forms the higher levels in the Gaussian pyramid. The spatial resolution reduces as we move up in the pyramid. This paper follows a top down multi resolution approach for filling the inpainting area which means the images are inpainted from the topmost level to the original image at the bottom of the pyramid. Since Gaussian pyramids do not preserve the structural information between the levels, Laplacian pyramids are considered. Laplacian pyramid is capable of synthesizing the original image from the top most images without any error. Apart from this it also segregates the structural information at each level. The technique in this paper utilizes the patch based Exemplar method as discussed by Crimsini et al in [25] which assigns priorities for pixel and reconstructs from the boundary looking for similar patches from the undamaged area. The nature of the pyramid together with the top down approach inherently reduces the inpainting area into many smaller regions at successive levels. This in turn enhances the performance of the algorithm. The paper is organized with the state of art in section II, the detailed discussion of the proposed method in section III, the experimentation and result in section IV and conclusion in section V.

## 2.STATE OF THE ART

In inpainting terminology, missing area or the damaged area is called as Ω, the known or undamaged area is termed as source Φ and the boundary between them is termed as δΩ as shown in fig. 1. The Ω will be specified as an input to the algorithm in the form of a binary

image called the mask. The inpainting algorithm should assign appropriate gray levels to the Ω such that it blends with the remaining image. The boundary δΩ, plays a major role in deciding the intensities in Ω. The existing inpainting algorithms are iterative and try to fill in the area near the δΩ until a criterion is reached.

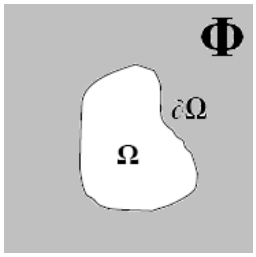


Fig.1. Digital image Inpainting problem

Interpolation methods [4],[7] are the primitive methods which can be used for inpainting. In the interpolation method, the neighboring pixels are considered for filling the inpainting area. The technique gives better result for the uniform area and fails in high structured regions. Bertalmio et al. [12], [18] used a digital image inpainting algorithm based on partial differential equations (PDEs). Anisotropic diffusion[2] is applied to extent the isophote lines. Though the algorithm works well for small textured images, it fails in large textured images. The mathematical models for variational PDE are explained in detail in [22]. In [13] a convolution mask is used to extend the gray levels in to the inpainting area. The curvatures are extended into the inpainting area in [14]. Level line based inpainting is discussed in [20]. Other methods involving partial differential equation and concentrating on smaller structures could be found in [10] and [23].

Texture based methods could be used for synthesizing images [8]. Various texture synthesis methods could be found from [9],[15],[16] and [19]. These methods grow a new image outward from an initial seed. Pyramid based texture synthesis are discussed in [3] and [6]. Texture synthesis based inpainting are used in [5] and [24]. Exemplar based technique for filling image regions are dealt in [17] and [25]. It is derived from patch based texture synthesis. The algorithm works by taking a patch around a pixel on the boundary and replacing it with the best patch found by searching in the source region. In [25] both structure and texture information is propagated into the mask region. Inpainting in a video sequence is discussed in [21] and fractal based method is discussed in [26].

A comparative analysis of structure and texture based methods is discussed in [27]. A hierarchical model using TV method is discussed in [28] which reproduces the general texture for a large mask but fails in reproducing finer details. A hierarchical model using wavelets is discussed in [30], though it reproduces the texture appropriately, it increases the overhead of inpainting in the four components for each level. A hierarchical exemplar based model is discussed in [29]. Hierarchical filling performs better in reproducing the structure and texture but

results in distortion due simple subsampling process. The advantage of hierarchical filling is used in this paper in an efficient way by segregating structure and texture with an overhead much less when compared to Wavelet based method.

## 3.INPAINTING USING LAPLACIAN PYRAMID

Image pyramids are suitable for multi resolution image processing. The general structure of image pyramid is shown in Fig.2 with the image of size *N* x *N*, at the base of the pyramid. The lower resolution images forms the higher layers of pyramid and the lowest resolution image at the apex. Generating the pyramid from the bottom is called as decomposition while generating from the top is called as synthesis. For hierarchical inpainting, the image and the area to be inpainted is represented at different resolution levels. The Inpainting algorithm is applied in a top down manner starting from the apex of the pyramid; the results are updated in the layer immediately below it. This process continues until the base image is inpainted. Usually the inpainting process uses only few layers from the base depending on the mask size.

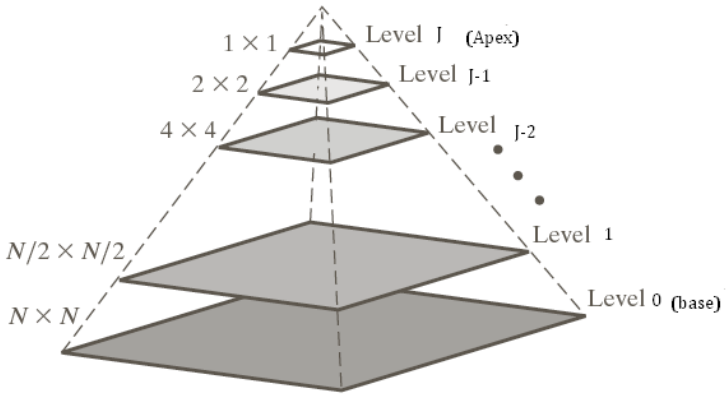


**Fig.2. Image Pyramid**

The main success of inpainting algorithm relies on the segregation of the structure and texture. A blurring process reduces the structural information in an image. When a sampling process is done on it, it forms the layers of a Gaussian pyramid. The difference of blurred version and the image is expected to give the structural information. This is generally called as the Laplacian. The loss of data between the levels should be minimal to avoid the additional error incurred by the sampling. Separating the structure from the texture and handling them individually improves the quality of the inpainting algorithm. These requirements makes the Laplacian pyramid a better choice. The Laplacian pyramid has the Gaussian image at the apex and the Laplacian images at other layers. Inpainting in Laplacian pyramid is carried out in two different ways depending on the Gaussian used for synthesizing. Another method using Gaussian and Laplacian at each level is also experimented.

### 3.1 Inpainting With One Gaussian

In the first method the image is blurred level number of times (say 'j') and each time it is down sampled and subtracted from the unblurred version to get the Laplacian. Finally the pyramid consists of Laplacian images with size varying from N x N at level 0 to $N/2^j$ x $N/2^j$ at level 'j'. It has a Gaussian image which is blurred 'j' times and is of size N x N. The mask pixels are extracted and maintained separately for each level. Inpainting algorithm is applied to the topmost Laplacian and the results are updated in the layer below. The algorithm stops after inpainting the Gaussian once and adding it to the base Laplacian.

In the second method, formation of the Laplacian pyramid remains the same as described before, but the Gaussian in this case is a single blurred version of the original image. Hence the pyramid consists of Laplacian images with size varying from N x N at level 0 to $N/2^j$ x $N/2^j$ at level 'j' and a Gaussian image which is blurred once and is of size N x N. Inpainting algorithm is similar to the previous method. Both the method described above introduces additional cost of inpainting the Laplacians at each level. Since the inpainting is done in a top down manner and the pixels inpainted at higher levels of pyramid are not repainted in the lower levels, the computational cost incurred due to multi resolution processing is thus reduced effectively. Moreover updating lower levels with the inpainted results of the higher level provides more interior pixel effectively breaking down the single large sized mask into many smaller sized ones. Many inpainting algorithms are efficient for smaller sized masks.

### 3.2 Inpainting With Multiple Gaussian

In this method the Gaussian and the Laplacian at each level is maintained in the pyramid. Hence the pyramid consists of 'j+1' Laplacian and 'j+1' Gaussian images. The images at the '$j^{th}$' level of the pyramid is of size $N/2^j$ x $N/2^j$. The algorithm inpaints top most layer of Gaussian and the Laplacian. The result of the Laplacian is updated to the layer below while their combined results are used to update the Gaussian in the layer below. The algorithm proceeds until the base level. This inpainting cost doubles when compared to the previous method, but the combination of structure and texture at each level result in better reconstruction.

### 3.3 Inpainting Algorithm

At each level of the pyramid Exemplar based inpainting is applied to the mask pixels. In this method a sub window called patch ($\psi_p$) centered on a pixel 'p' at $\delta\Omega$ is chosen for inpainting. This sub window encompasses certain pixels from $\Phi$ and certain other pixels from $\Omega$. The source region ($\Phi$) is queried for similar pixels as that of known pixels in the sub window. The closest match provides the values for the unknown pixels in the patch. The Boundary $\delta\Omega$ and the mask pixels $\Omega$ are updated and the process continues until all mask pixels are assigned values. The process of Exemplar based inpainting is illustrated in Fig. 3. The selection of patches plays a crucial role in the quality of inpainting. The presence of more known pixels and the patch centered on a structure are primary concern in the selection process. The Confidence term C(p) and the Data term D(p), as coined by Crimsini et al[25]. are used for this purpose.

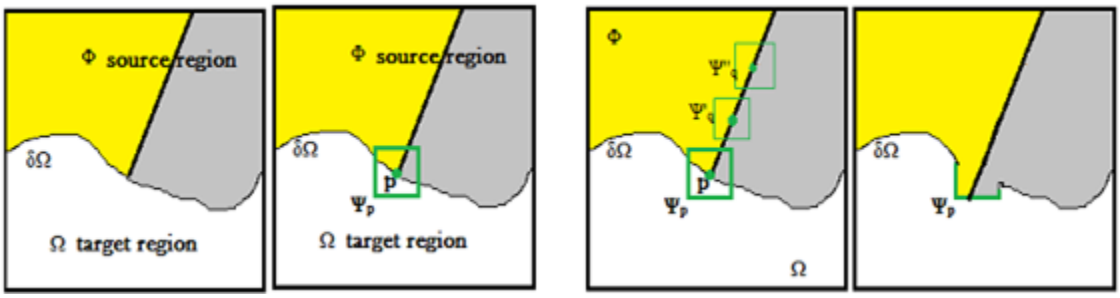


Fig.3. Exemplar based Inpainting

The algorithm for Laplacian pyramid based hierarchical inpainting is as follows:

1. Accept the area to be inpainted(mask) from the user through color, area selection or mask file
2. Generate the Pyramid as specified in section 3.1 and 3.2
3. Compute the mask pixels at each layer.
4. Initialize the confidence term for the mask pixels to zero.
5. Compute the priority of the patches of the top most layer as given by Eqn (1)

$$P(p) = C(p) * D(p) \quad (1)$$

Where C(p) and D(p) refers to the confidence term and data term of the patch ($\psi_p$) centered at pixel 'p'. They are calculated using Eqn(2) and Eqn(3) respectively

$$C(p) = \frac{\sum_{q \in \psi_p \cap \Omega} C(q)}{|\psi_p|} \quad (2)$$

Where $|\psi_p|$ is the cardinality of the patch.

$$D(p) = \frac{|\nabla p^{\perp} . np|}{\alpha} \quad (3)$$

Where $\nabla p^{\perp}$ is the isophote which is orthogonal to the gradient $\nabla p$ , $\alpha$ is the normalization factor, np is the normal vector to the contour $\delta\Omega$ at p

6. Choose the patch Ψp with the maximum priority as in equation (4),

$$p = arg\ max\ p\ for\ all\ P(p) \quad (4).$$

7. Find the best matching patch Ψq Є Φ in source region that minimizes d(Ψ p; Ψ q), where d is the Sum of Squared Distance(SSD).
8. Copy image data from Ψ q to Ψ p for all pixels belonging to the target region Ω.
9. Update *C*(p) and the D(p) for the newly filled pixels.
10. Repeat steps 5 to 9 until all target pixels in the current level are filled.
11. Update the pixel values in the layer below and update the mask pixels.
12. Repeat step 4 to 11 until the base of the pyramid is inpainted.

## 4. EXPERIMENTAL RESULTS

Images consisting of different textures and structures are considered for experimentation. Isotropic diffusion based methods perform well in smooth areas; anisotropic diffusion based methods and Partial differential equation based method perform well for smaller inpainting regions but fail for larger inpainting area. Texture synthesis based methods perform well for larger regions but fails to propagate the structure. Exemplar based method performs well in natural images but fails in larger structure propagation. The performance of inpainting with multiple Laplacian and Gaussian is compared with the existing method for a textured image in Fig 4. The left most image represents the image with a large mask and the results of anisotropic diffusion method, Total variation method, exemplar based method and the proposed method are listed to its right in the order specified.

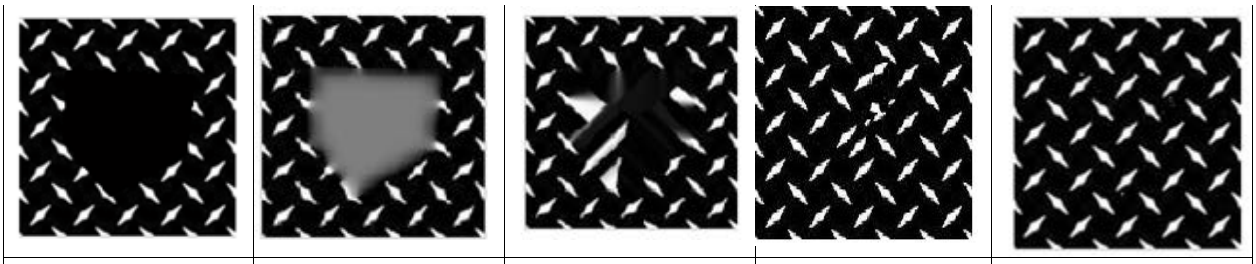

| (a)Image with mask | (b)Anisotropic diffusion | (c)Total variation | (d)Exemplar | (e) Multiple Laplacian |
|---|---|---|---|---|

Fig. 4 : Comparison with existing methods

The result of exemplar based method on a natural image is shown in Fig. 5a. A similar image with the mask area in white color is shown in Fig 5b. The result of a hierarchically inpainted image is shown in Fig 5c. The result of inpainting using Gaussian pyramid upto 2 levels is shown in Fig.6. The image with mask and the inpainted result from first and second level are shown in the order from left to right.


| (a). Exemplar based method | (b). Similar image with mask | (c). Hierarchically inpainted |
|---|---|---|

Fig. 5 : Comparison of exemplar method with hierarchical method

It is clear from the picture that its performance drops as we move up in the pyramid. The method using single Gaussian had varied response among different images. When the Gaussian that is blurred j times and all the Laplacians were used, the images with linear structures were not constructed properly, the overall texture construction was better. It also reduced the sharpness in a reconstructed image. The results on various images are shown in Fig 7(a) through (e). When all the Laplacians and the original image was used for inpainting the blurring was avoided but the overall reconstruction in a textured image was not upto the mark. Some of the results on similar images are shown in Fig 8 (a) through (e).

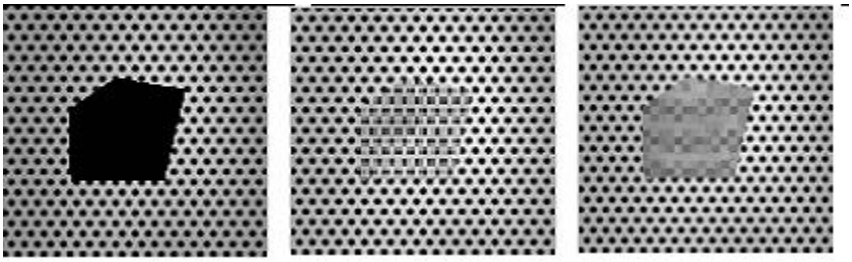

**Fig. 6 : Inpainting with Gaussian Pyramid**

(a) (b) (c) (d) (e)

**Fig. 7(a)-(e) : Inpainting using single Gaussian (blurred)**

(a) (b) (c) (d) (e)

**Fig.8(a)-(e) : Inpainting using single Gaussian (Original)**

When the Laplacian and Gaussian at each level are inpainted separately and their combined results were updated to the lower level in the pyramid, the structure and texture reconstruction was better. The result of Inpainting the Laplacian and Gaussian at each level for an image is shown in Fig 9. The area is selected by the user for inpainting. The number of levels were fixed as 3 for this case. The Gaussian and Laplacian are inpainted at level three and given as input to level 2, where some portions are inpainted and given to level 1 as illustrated in

Fig.10. Though the images are of different size they are shown in same scale for ease of comparison.

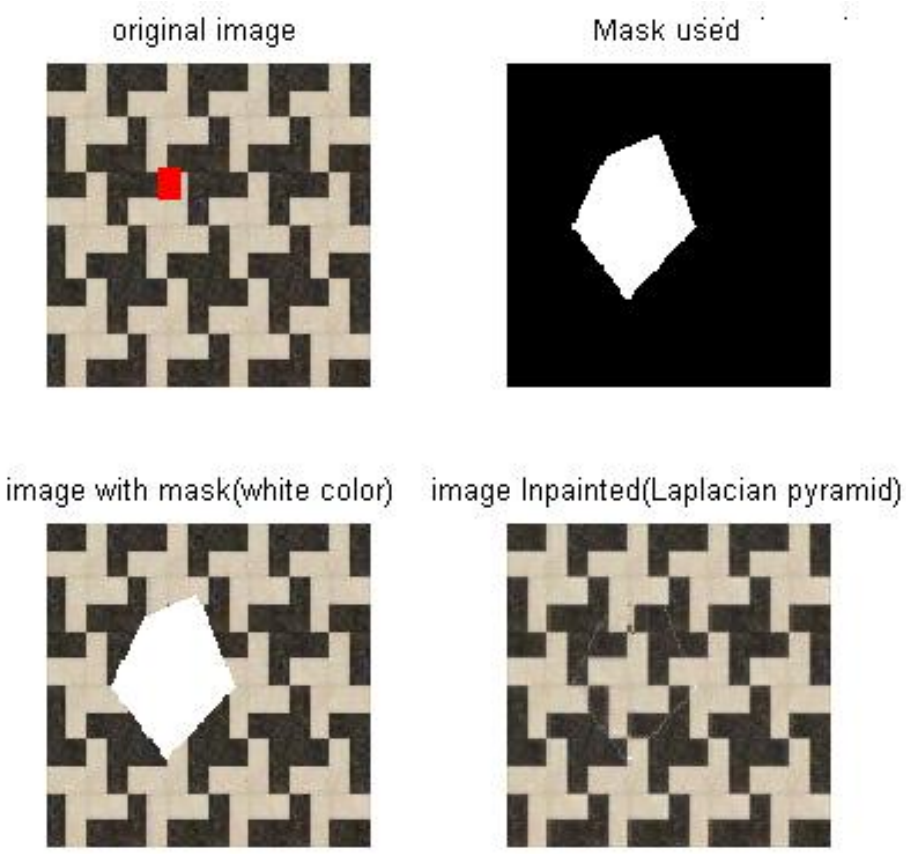


Fig.9 : Inpainting using multiple Gaussian

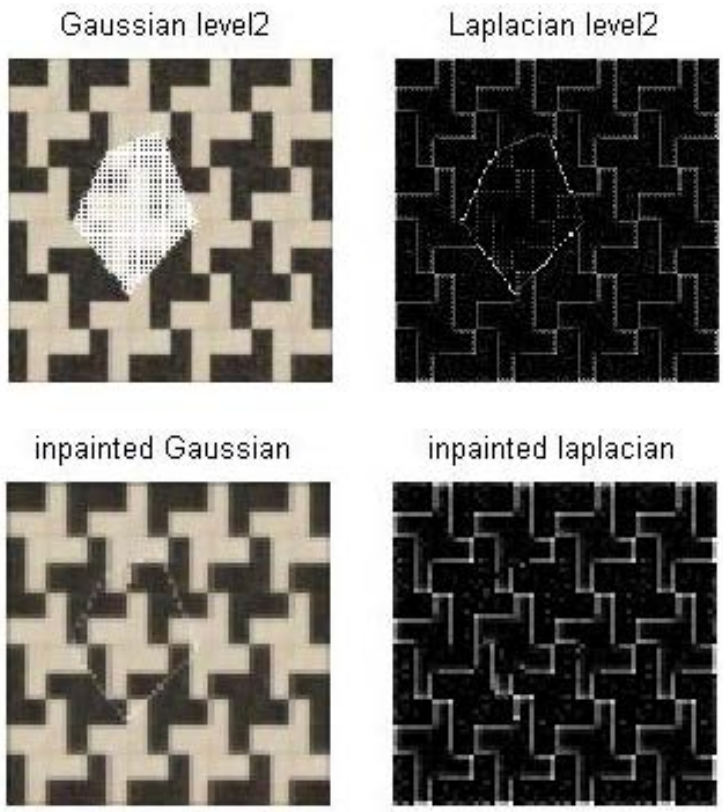


Fig. 10 : Inpainting using multiple Gaussian atLevel 2

The Size and the spread of the Gaussian filter used for generating the pyramid also contributes to the quality of the reconstructed image. The reconstructed images with various window sizes and spreads are shown in Fig. 11. The reconstructed image with window size 5x5 and spread of 0.3 is shown in Fig.11a; window size 5x5 and spread 0.9 in Fig11b; window size 9x9 and spread 0.5 in Fig11c and window size 9x9 and spread 0.9 in Fig11d.

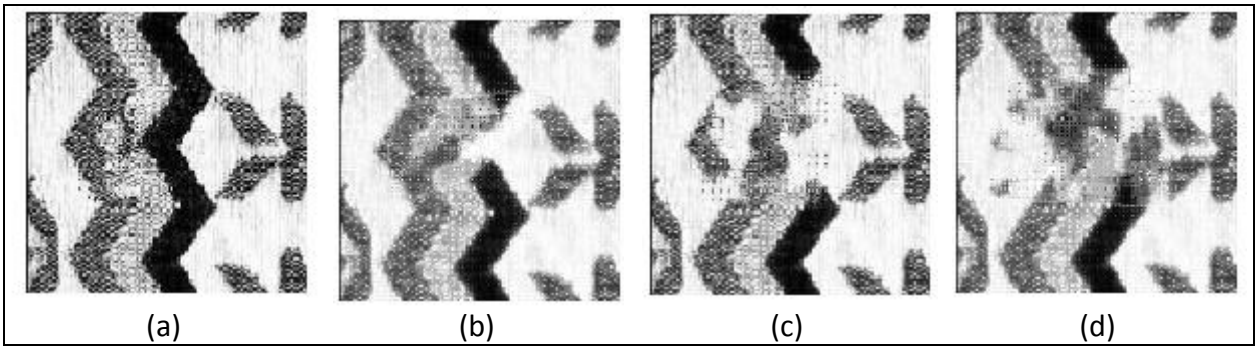


Fig. 11 (a)-(d): Inpainted images with various window size and Spread

As the spread increases the blurring in the reconstructed image also increases. When the window size increases the larger structures are reconstructed properly but it may introduce noisy textures whose visibility is less in a natural scenary images but is clearly visible in fixed shape images. Smaller window sizes degrades the structure reconstruction and also introduces the noisy textures in fixed shape images. The Choice of the window size is majorly influenced by

the nature of the image. For the test data that has been considered a spread of 0.5 and a window size of 5x5 gave good results. The number of levels used for inpainting is influenced by the size of the area to be inpainted. Inpainting upto level 3 proved sufficient for the data set. The rectangular patch being considered affects the all exemplar based inpainting while inpainting curved areas. The effects are predominant for images with few fixed shapes and colors. The result of inpainting an oval area is shown in Fig 12 (b)-(f). The original image with the area to be inpainted indicated in black is shown in Fig12(a). The inpainted image using Exemplar based method, Laplacian pyramid with blurred Gaussian, Laplacian pyramid with unblurred Gaussian, Laplacian pyramid with multiple Gaussians with 5x5 window size, 0.3 spread and 9x9 window size, 0.5 spread is shown in Fig 12 (b),(c),(d),(e) and (f) respectively.

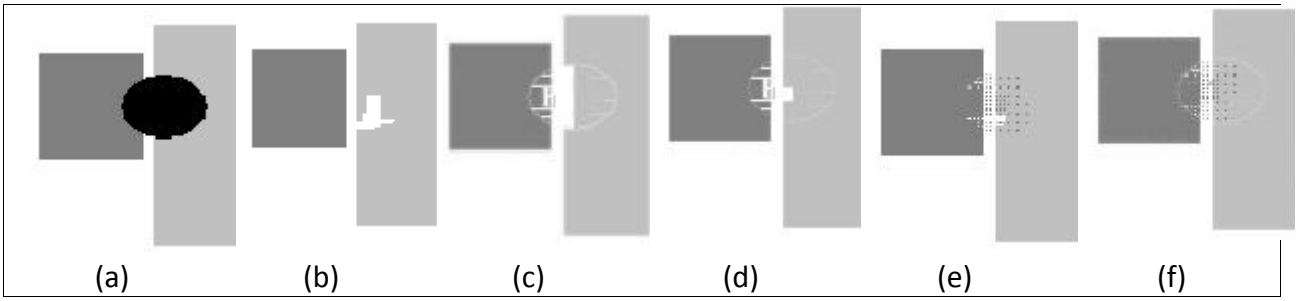


Fig. 12 (b)-(f): Exemplar based Inpainted images for Oval area shown in (a)

## 5. CONCLUSION

Inpainting an image requires the proper reconstruction of the structures and textures. Parital Differential equation based methods fail for larger inpainting areas. Texture synthesis based methods does not guarantee the completion of structures. The existing exemplar based algorithms fail in reconstructing larger structure and depends on the boundary pixels for filling the regions. The error occurring in the initial stage percolates to the interior regions. When inpainted using a Laplacian pyramid the structural and textural information are handled separately. Inpainting in a top down manner reduces the mask size at successive levels giving more known interior pixels which increases the performance of the Exemplar based method. A combination of structure and texture at each level is required for a perfect reconstruction though it consumes more time than inpainting the laplacians and a single Gaussian. The window size and the spread of the filter and the number of levels in the pyramid affect the inpainting quality and the computational cost. The choice of these parameters is influenced by the nature of the image and the size of the mask. The Laplacian pyramid based inpainting introduces noise at lower pyramids when the mask area is oval and when the image has few definite shapes. Exemplar based methods are limited in synthesizing the image portions that are existing in the surrounding and do not generate any new patterns.

## REFERENCES

[1]. P.J. BURT, E. H. ADELSON.,"The Laplacian Pyramid as a Compact Image Code"., IEEE Trans on Communication,vol. COM-31, no. 4, April 1983

[2]. P. PERONA AND J. MALIK, Scale-Space Edge Detection Using Anisotropic Diffusion, *IEEE Transactions on Pattern Analysis and Machine Intelligence, Vol. 12, No.7, July 1990,* http://www.cs.berkeley.edu/~malik/papers/MP-aniso.pdf

[3]. D.J. HEEGER AND J.R. BERGEN, Pyramid-Based Texture Analysis/Synthesis, *Proceedings of SIGGRAPH 1995, pp 229-238, September 1995.*http://www.cns.nyu.edu/~david/ftp/reprints/heeger-siggraph95.pdf

[4]. A.C. KOKARAM, R.D. MORRIS, W.J. FITZGERALD AND P.J.W. RAYNER, “Interpolation of Missing Data in Image Sequences”,IEEE Transactions on Image Processing. Vol. 4. No.11, Nov. 1995, pp 1509-1519. URL: http://www.robinmorris.org/sigproc/interpolation.pdf

[5]. H. IGEHY AND L. PEREIRA, “Image Replacement through Texture Synthesis”,Proceedings of the IEEE International Conference on Image Processing, October 1997.URL: http://graphics.stanford.edu/papers/texture_replace/texture_replace.pdf

[6]. J.S. DE BONET, “Multi resolution sampling procedure for analysis and synthesis of texture images”, in Proc. ACM Conference Computer Graphics (SIGGRAPH), volume 31, pages 361–368, 1997.

[7]. V. CASELLES, J. M. MOREL, AND C. SBERT, "An Axiomatic Approach to Image Interpolation", IEEE Transactions on Image Processing, 7, Issue 3, Mar 1998, Page(s): 376 - 386.

[8]. M. TUCERYAN AND A. K. JAIN, “Texture Analysis,” Handbook of Pattern Recognition and Computer Vision, C. H. Chan, L. F. Pau, and P. S. P. Wang (Eds.), Ch.2, pp. 235-276, Singapore: World Scientific, 1998.

[9]. A. EFROS AND T. LEUNG. Texture synthesis by non-parametric sampling.In *Proc. Int. Conf. Computer Vision*, pages 1033–1038, Kerkyra, Greece, September 1999.

[10]. M. BERTALMIO, G. SAPIRO, V. CASELLES, AND C. BALLESTER, "Image Inpainting" Proceedings of the ACM SIGGRAPH Conference on Computer Graphics, SIGGRAPH2000, New Orleans, USA. July 2000, pp 417-424. URL: http://www.iua.upf.es/~mbertalmio/bertalmi.pdf

[11]. M. BERTALMIO, A.L. BERTOZZI AND G. SAPIRO, “Navier-Stokes, Fluid Dynamics, and Image and Video Inpainting”, Proc. IEEE Computer Vision and Pattern Recognition (CVPR’01), Hawaii, December 2001. http://www.iua.upf.es/~mbertalmio/final-cvpr.pdf

[12]. BALLESTER, M. BERTALMIO, V. CASELLES, G. SAPIRO, AND J. VERDERA, "Filling-in by Joint Interpolation of Vector Fields and Gray Levels", IEEE Transaction on Image Processing, 10, Issue 8, Aug 2001, Page(s): 1200 - 1211.

[13]. M.M. OLIVIEIRA, B. BOWEN, R. MCKENNA AND Y.S. CHUNG, “Fast Digital Image Inpainting”, Proceedings of the International Conference on Visualization, Imaging and Image Processing (VIIP 2001), Marbella, Spain 2001. Sep. 3-5, 2001, pp 261-266. URL: http://www.cs.sunysb.edu/~oliveira/pubs/inpainting.pdf

[14]. T. F. CHAN AND J. SHEN, "Non-Texture Inpainting by Curvature-Driven Diffusions (CDD)", Journal Visual Communication and Image Representation, 12, Number 4, 2001, Page(s): 436 - 449.

[15]. M. ASHIKHMIN. “Synthesizing natural textures”. In Proc. ACM Symposium on Interactive 3D Graphics, pages 217–226, Research Triangle Park, NC, March 2001.

[16]. A. EFROS and W.T. FREEMAN, “Image quilting for texture synthesis and transfer”. In Proc. ACM Conf. Comp. Graphics (SIGGRAPH), pages 341–346, Eugene Fiume, August 2001.

[17]. A. HERTZMANN, C. JACOBS, N. OLIVER, B. CURLESS, and D. SALESIN, “Image analogies”. In Proc. ACM Conf. Comp. Graphics (SIGGRAPH), Eugene Fiume, August 2001.

[18]. C. BALLESTER, V. CASELLES, J. VERDERA, M. BERTALMIO, and G. SAPIRO. “A variational model for filling-in gray level and color images”. In Proc. Int. Conf. Computer Vision, pages I: 10–16, Vancouver, Canada, June 2001.

[19]. P.Harrison, “A non-hierarchical procedure for re-synthesis of complex texture”, in Proc. Int. Conf. Central Europe Computer Graphics, Visualization And Computer Vision, Plzen, Czech Republic, February 2001.

[20]. S. MASNOU, "Disocclusion: A Variational Approach using Level Lines", IEEE Transactions on Signal Processing, 11, Issue 2, Feb 2002, Page(s): 68- 76.

[21]. R. BORNARD, E. LECAN, L. LABORELLI AND J-H. CHENOT, “Missing Data Correction in Still Images and Image Sequences”, ACM Multimedia 2002, Juan-les-Pins, France, Dec. 2002. URL: http://brava.ina.fr/papers/INA_Raphael_Bornard/RBornard_mm2002_preprint.pdf

[22]. T.F. CHAN, J. SHEN AND L. VESE, “Variational PDE Models in Image Processing”, UCLA Computational and Applied Mathematics Reports 02-61, Dec. 2002. URL: ftp://ftp.math.ucla.edu/pub/camreport/cam02-61.pdf

[23]. J. SHEN, “Inpainting and the Fundamental Problem of Image Processing”, SIAM News 36(5), June 2003. http://www.math.ucla.edu/~imagers/htmls/internalreport/ShenSIAM.pdf

[24]. M. BERTALMIO, L. VESE, G. SAPIRO AND S. OSHER, “Simultaneous Structure and Texture Image Inpainting”, in Proc. Conference Computer Vision Pattern Recognition, Madison, WI, 2003. Proceedings of the 2003 IEEE Computer Society Conference on Computer Vision and Pattern Recognition (CVPR’03), volume 2, June 2003. URL: http://www.math.ucla.edu/~lvese/PAPERS/01211536.pdf

[25]. A. CRIMINISI, P. PÉRES AND K. TOYAMA, "Region Filling and Object Removal by Exemplar-Based Image Inpainting"., IEEE Trans on Image Processing , vol. 13, NO. 9, sep 2004

[26]. I. DRORI, D. COHEN-OR AND H. YESHURUN, “Fragment-Based Image Completion”, ACM Transactions on Graphics (TOG), volume 22 issue 3, July 2003. URL: http://portal.acm.org

[27]. S.PADMAVATHI, K.P.SOMAN ,Comparative Analysis of Structure and Texture based Image Inpainting Techniques, International Journal of Electronics and Computer Science Engineering,( IJECSE )Volume 1, Number 3, June 2012, pp1062-1069

 

[28]. S.PADMAVATHI, N.ARCHANA, K.P.SOMAN , Hierarchical Approach For Total Variation Digital Image Inpainting, International Journal of Computer Science, Engineering and Applications (IJCSEA), Volume 2, number 3, june 2012, PP173-182

[29]. S.PADMAVATHI, K.P.SOMAN, A Hierarchical Search Space Refinement and filling for Exemplar based Image Inpainting, International Journal of Computer Applications (IJCA) Volume 52, number4, August 2012, pp31-37.

[30]. S.PADMAVATHI, B. PRIYA LAKSHMI, K.P.SOMAN, Hierarchical Digital Image Inpainting using Wavelets , Signal & Image Processing:An International Journal (SIPIJ),Volume 3, Number 4, August 2012, pp85-93.

AIVP ADVANCES IN IMAGE AND VIDEO PROCESSING

SOCIETY FOR SCIENCE AND EDUCATION UNITED KINGDOM

VOLUME 2, ISSUE 1
ISSN: 2054 - 7412

# Qualitative and Quantitative Analysis of Non-Uniform Dark Images

**Priti Rajput[1], Sandeep Arya[2], Santoresh Kumari[3], Parveen Lehana[2]**
[1]*Directorate of Economics & Statistics, J&K, India*
[2]*D.S.P. Lab, Dept. of Physics & Electronics, University of Jammu, J&K, India*
[3]*Dept. of Computer Science, MIET Jammu, J&K, India*
*Email: pklehanajournals@gmail.com, snp09arya@gmail.com*

**ABSTRACT**

In this paper, an algorithm is developed to attain information from the dark images and an analysis is sought for the impact of brightness adjustment parameter (α) and color hue (λ) on a single dark image. The algorithm appears quite appealing as the quality of the images become clearer. This algorithm is applied on a single dark image for different values of α and λ and out of resultant twenty four images; medium, high and low quality were selected randomly for mean opinion score. A mean score opinion (MOS) is drawn for a set of processed and unprocessed images and the results gathered shows that the processed image gathers valuable information and appeared clear. Results showed that few parts where no information was being noticed before processing the digital image, now provides information to the subject after processing..

Keywords: Digital image processing, enhancement, image quality, MOS, image analysis.

## 1.INTRODUCTION

Digital image processing possess their application in intelligent transportation systems such as automatic number plate recognition, traffic sign recognition, weather forecasting, and in medical field for diagnosis of diseases, satellite systems, remote areas , space research etc [1]. The high quality of an image is the prime requirement and is possible to obtain using image enhancement techniques. There is no such theory of image enhancement. It's a visual perception [2] [3]. Several enhancement techniques exist and few of them work on dark images and some on day light images. Thus the field of image enhancement techniques provides a significant ways to modify specific set of images suitable for the concerned user [4]. Image enhancement is the method to enhance the quality of images in term of contrast, brightness and sharpness [5-8]. The objective of image enhancement is to enhance the image so that the processed image is more suitable for a particular set of application [2-4] [9-23]. Enhancing the digital image can be done in various ways [24]. All depends upon the viewer's perception or

**DOI**: 10.14738/aivp.21.45
**Publication Date:**10th February 2014
**URL**: http://dx.doi.org/10.14738/aivp.21.45

interpretability to access the image [2] [25]. Some applications require removing the noise and in others may be brightening the dark images are the prime requirement. Researchers had classified the image enhancement techniques into two categories; Spatial domain methods and frequency domain methods [2-3] [15] [18] [22-23] [26-29] [30-32].

Spatial domain refers to the aggregate of pixels composing an image, i.e., pixel values are manipulated to obtain a better enhanced image. It directly deals with changing the individual pixel values and hence the contrast value of the whole image [15] [18]. The frequency domain method deals with the manipulation of the orthogonal transform of the image i.e., it deals with the image indirectly. Magnitude and phase are the main components of orthogonal transform [20] [22] [23]. Magnitude deals with the frequency content and phase is to restore the image back to the spatial domain. All the image enhancement operations are carried on the Fourier transform of the image and then the inverse Fourier transform is carried to obtain the resultant image [2-3] [20] [22-23] [26-28] [30-33].

Though a number of techniques exist for colour image enhancement, we in this paper, concentrated on image enhancement of dark images only. The dark images can be brightened by power law transformations or log transformations. The power law transformation expands the gray level thus capturing information from dark regions whereas the log transformations brighten the dark regions at the expense of brighter region information [2-3] [20] [22-23] [26-28] [30-32]. Here we have used the enhancement technique purposed by Sertan Erkanli et al for capturing information from the low quality images [34-36]. They proposed the enhancement technique for non-uniform and uniform dark images (ETNUD).

## 2. TRANSFORMATION PARAMETERS

According to Sertan Erkanli et al, the intensity *I* of the color image is provided by the equation *I*(*m,n*) and is given as

$$I(\mathrm{m},\mathrm{n}) = 0.2989\mathrm{R}(\mathrm{m},\mathrm{n}) + 0.587\mathrm{G}(\mathrm{m},\mathrm{n}) + 0.114\mathrm{B}(\mathrm{m},\mathrm{n})$$

where R, G, B are the red, green and blue components of the color image. For *I* having 8-bits per pixel, $I_n$ is the normalized version of *I*, such that

$$I_{\mathrm{n}}(\mathrm{m},\mathrm{n}) = \frac{I(\mathrm{m},\mathrm{n})}{255}$$

Researchers analyzed that the linear input-output intensity relationships does not provide good visual perception as compared to that of direct viewing of the scene. To get a better perception, nonlinear transformation for dynamic range compression is used.

Several enhancement methods are based on center/surround ratios. Gaussian form is one such method to produce good dynamic range compression. The luminance of surrounding pixels using 2D discrete spatial convolution with a Gaussian kernel is given as,

$$G(m,n) = K \exp\left(-\frac{m^2+n^2}{\sigma_s^2}\right)$$

where $\sigma_s$ is the surround space constant equal to the standard deviation of $G(m,n)$ and $K$ is determined under constraint that $\sum_{m,n} G(m,n) = 1$.

An adaptive contrast enhancement parameter (S) related to the global deviation of the input intensity image, $I(m,n)$, and '$*$' as the convolution operator, is defined as

$$S = \begin{Bmatrix} 3 \ \ for \ \ \sigma \le 7 \\ 1.5 \ \ for \ \ 7 < \sigma \le 20 \\ 1 \ \ for \ \ \sigma \ge 20 \end{Bmatrix}$$

$\sigma$ is the contrast- standard deviation of the original intensity image. If $\sigma<7$, the image has poor contrast and contrast of the image will be increased. If $\sigma \ge 20$ the image has sufficient contrast. These are the factors responsible for the enhancement of the information or images or in other words refining the digital image. The quality of the digital image can be calculated as

$$Q = 0.5\mu_n + 0.4\,\sigma_n + 0.1S$$

where $\mu_n$ is the normalized brightness parameter, $\sigma_n$ is the normalized contrast parameter, and $S$, the sharpness.

**Table 1. Quality of processed images for different combinations of α and λ.**

| α | λ | | | | | | | | | | |
|---|---|---|---|---|---|---|---|---|---|---|---|
| 0.00 | 0.15 | 0.25 | 0.35 | 0.45 | 0.50 | 1.00 | 2.00 | 3.00 | 4.00 | 6.00 | 7.00 |
| -0.80 | 0 | 0 | 0 | 0 | 0 | 0 | 1 | 1 | 1 | 1 | 1 |
| -0.75 | 0 | 0 | 0 | 0 | 0 | 0 | 1 | 1 | 1 | 1 | 1 |
| -0.70 | 0 | 0 | 0 | 0 | 0 | 0 | 1 | 1 | 1 | 1 | 1 |
| -0.65 | 0 | 0 | 0 | 0 | 0 | 1 | 1 | 1 | 1 | 1 | 1 |
| -0.60 | 0 | 0 | 0 | 0 | 0 | 1 | 1 | 1 | 1 | 1 | 1 |
| -0.55 | 0 | 0 | 0 | 0 | 0 | 1 | 1 | 0 | 0 | 0 | 0 |
| -0.50 | 0 | 0 | 0 | 0 | 0 | 1 | 0 | 0 | 0 | 0 | 0 |
| -0.45 | 0 | 0 | 0 | 0 | 1 | 1 | 0 | 0 | 0 | 0 | 0 |
| -0.40 | 0 | 0 | 0 | 0 | 1 | 1 | 0 | 0 | 0 | 0 | 0 |
| -0.35 | 0 | 0 | 0 | 1 | 1 | 1 | 0 | 0 | 0 | 0 | 0 |
| -0.30 | 0 | 0 | 0 | 1 | 1 | 1 | 0 | 0 | 0 | 0 | 0 |
| -0.25 | 0 | 0 | 0 | 1 | 1 | 1 | 0 | 0 | 0 | 0 | 0 |
| -0.20 | 0 | 0 | 0 | 1 | 1 | 0 | 0 | 0 | 0 | 0 | 0 |
| -0.15 | 0 | 0 | 0 | 1 | 1 | 0 | 0 | 0 | 0 | 0 | 0 |
| -0.10 | 0 | 0 | 1 | 1 | 1 | 0 | 0 | 0 | 0 | 0 | 0 |
| -0.05 | 0 | 0 | 1 | 1 | 1 | 0 | 0 | 0 | 0 | 0 | 0 |
| 0.00 | 0 | 0 | 1 | 1 | 1 | 0 | 0 | 0 | 0 | 0 | 0 |
| 0.05 | 0 | 0 | 1 | 1 | 1 | 0 | 0 | 0 | 0 | 0 | 0 |
| 0.10 | 0 | 0 | 1 | 1 | 1 | 0 | 0 | 0 | 0 | 0 | 0 |
| 0.15 | 0 | 0 | 1 | 1 | 1 | 0 | 0 | 0 | 0 | 0 | 0 |
| 0.20 | 0 | 0 | 1 | 1 | 1 | 0 | 0 | 0 | 0 | 0 | 0 |
| 0.25 | 0 | 0 | 1 | 1 | 1 | 0 | 0 | 0 | 0 | 0 | 0 |
| 0.30 | 0 | 0 | 1 | 1 | 1 | 0 | 0 | 0 | 0 | 0 | 0 |
| 0.35 | 0 | 0 | 1 | 1 | 1 | 0 | 0 | 0 | 0 | 0 | 0 |
| 0.40 | 0 | 0 | 1 | 1 | 1 | 0 | 0 | 0 | 0 | 0 | 0 |
| 0.45 | 0 | 0 | 1 | 1 | 1 | 0 | 0 | 0 | 0 | 0 | 0 |
| 0.50 | 0 | 0 | 1 | 1 | 1 | 0 | 0 | 0 | 0 | 0 | 0 |
| 0.55 | 0 | 0 | 1 | 1 | 1 | 0 | 0 | 0 | 0 | 0 | 0 |
| 0.60 | 0 | 0 | 1 | 1 | 1 | 0 | 0 | 0 | 0 | 0 | 0 |
| 0.65 | 0 | 1 | 1 | 1 | 1 | 0 | 0 | 0 | 0 | 0 | 0 |
| 0.70 | 0 | 1 | 1 | 1 | 1 | 0 | 0 | 0 | 0 | 0 | 0 |
| 0.75 | 0 | 1 | 1 | 1 | 1 | 0 | 0 | 0 | 0 | 0 | 0 |
| 0.80 | 0 | 1 | 1 | 1 | 1 | 0 | 0 | 0 | 0 | 0 | 0 |

## 3.METHODOLOGY

An image taken in dark provides little information or no information at all. The proposed algorithm refined the information present in the dark area. The evaluation criterion starts by taking a single dark image and then processing for different values of α and λ. More than 350 images were processed for different combinations of α and λ. The quality of the processed and unprocessed images was evaluated by resizing and selecting random pixel points of the image. For some processed images, the quality shows a high value but the picture clarity was poor. The reason is that the quality is controlled by three parameters contrast ($\sigma$), brightness ($\mu$) and sharpness ($S$). The value of μn should lie between 0.4 and 0.6. If this value alters, the quality value becomes numerically high but not visually. That's why in certain cases, the quality shows high calculated value but not visually. Similarly, the contrast value should lie between 0.25 and 0.5.

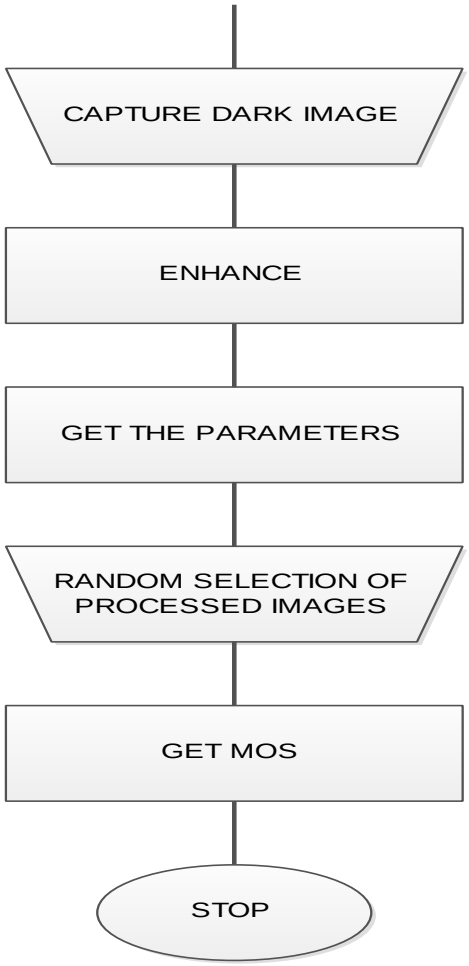


Figure 1: Flow chart showing the process to check for the MOS for assessment of the quality.

A random selection of 24 processed images was made besides one unprocessed image. Out of them, 8 were of high quality, 8 of low and 8 of medium quality. These images were then randomly selected and assessed for the quality of the digital images by ten different subjects. The subjects were unaware of the original and the processed images. Corresponding to each image, the marks out of ten were given by the subjects to the image. In other words, the mean score opinion (MOS) was noticed for each image. The average marks given by the ten evaluators were calculated and correspondingly quality and standard deviation is noticed. The results show interesting features.

The images were taken by 9.1 mega pixel digital camera in the evening time. About 50 different dark images were clicked and out of them, one with the darkest of all was selected to carry out the experiment. The selected image contained all the three primary colors shown in fig. 2.

Figure 2: Unprocessed Dark image.

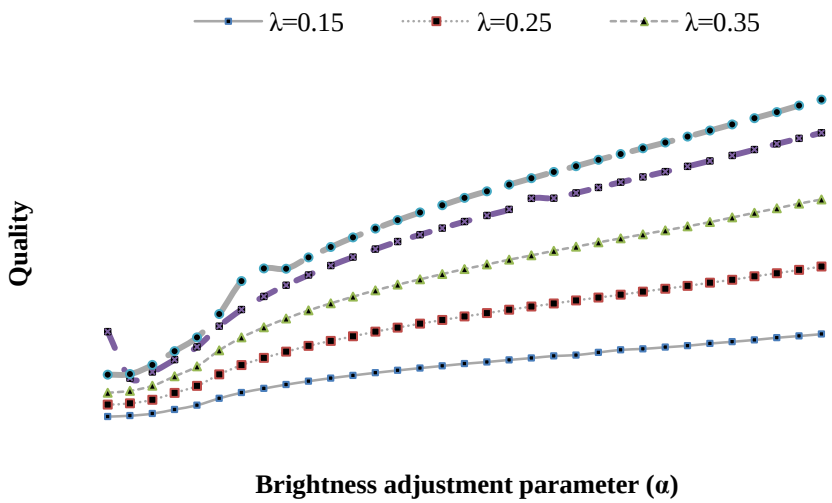


Figure 3: Quality curve for fractional values of λ.

The image has a quality factor of 0.3422 and a standard deviation of 0.002. A careful visual observation shows some missing information in the lower part of the image. This image is processed 385 times for different combinations of α and λ. Table 1 shows the processed quality results. The 0's in the table signifies that the images having quality lower than the original image and for 1's higher is the quality. The corresponding graphs are drawn for two set of λ; one having fractional values and other having integer values. The images corresponding to $\lambda \leqslant 0$ were not processed as they provide no information at all. Fig. 3 shows the graph for fractional values of $\lambda$. The alpha is taken from -0.80 to 0.80 with an auto increment of 0.05. As we go on increasing the $\alpha$ and λ the quality shows a hike in its values for fractional λ. Fig. 4 shows the graphs for integer values.

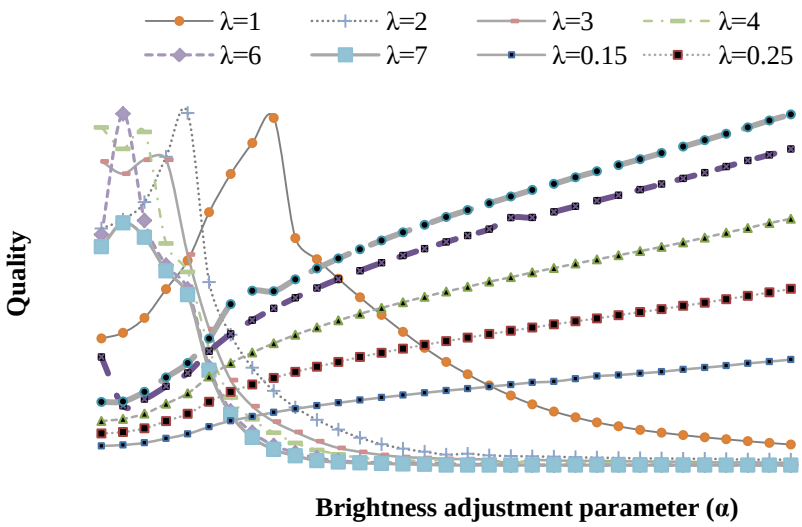


Figure 4: Quality curve for integer values of λ.

Here the results are quite interesting but opposite to that of the fractional λ. With the increase in α, the quality also shows an increase up to a certain value and then decreases in its value which saturates at about 0.2. This is impossible to show all the twenty four processed images. Fig. 5, Fig. 6, Fig. 7, and Fig. 8 shows the processed images out of 24 randomly selected images for MOS.

Figure 5: Processed image having α = -0.1 and λ = 1.

**Table 2. Quality and standard deviation of 24 randomly selected images for MOS.**

| α | λ | | | | | | | | | | | | | | | |
|---|---|---|---|---|---|---|---|---|---|---|---|---|---|---|---|---|
| | 0.25 | | 0.35 | | 0.45 | | 0.50 | | 1.00 | | 2.00 | | 3.00 | | 4.00 | |
| | Q | SD | Q | SD | Q | SD | Q | SD | Q | SD | Q | SD | Q | SD | Q | SD |
| -0.45 | | | | | | | | | | | 0.2853 | 0.0024 | | | 0.2401 | 0.0025 |
| -0.40 | | | | | | | | | 0.5038 | 0.0020 | | | 0.2290 | 0.0022 | 0.2284 | 0.0020 |
| -0.35 | | | | | | | | | | | 0.2505 | 0.0024 | | | | |
| -0.25 | | | | | | | 0.3809 | 0.0007 | 0.3630 | 0.0016 | | | | | | |
| -0.20 | | | | | | | 0.3889 | 0.0006 | 0.3468 | 0.0016 | | | | | | |
| -0.15 | | | | | | | 0.3966 | 0.0007 | | | | | | | | |
| -0.10 | | | | | | | 0.4037 | 0.0007 | 0.3166 | 0.0014 | | | | | | |
| -0.05 | | | 0.3473 | 0.0004 | | | 0.4103 | 0.0006 | | | | | | | | |
| 0.00 | 0.3085 | 0.0003 | 0.3519 | 0.0004 | | | | | | | | | | | | |
| 0.05 | | | | | 0.4009 | 0.0005 | 0.4231 | 0.0006 | 0.2794 | 0.0011 | | | | | | |
| 0.10 | | | 0.3605 | 0.0003 | | | | | | | | | | | | |
| 0.20 | | | 0.3686 | 0.0003 | 0.4167 | 0.0003 | | | | | | | | | | |
| 0.30 | | | 0.3763 | 0.0002 | | | | | | | | | | | | |

**Figure 6: Processed image having α = 0 and λ = 0.35**

**Table 3. Mean opinion score (MOS) given by 10 different users.**

| SUBJECTS | PROCESSED IMAGES | | | | | | | | | | | | | | | | | | | | | | | ORIGINAL IMAGE |
|---|---|---|---|---|---|---|---|---|---|---|---|---|---|---|---|---|---|---|---|---|---|---|---|---|
| | 1 | 2 | 3 | 4 | 5 | 6 | 7 | 8 | 9 | 10 | 11 | 12 | 13 | 14 | 15 | 16 | 17 | 18 | 19 | 20 | 21 | 22 | 23 | 24 | 25 |
| 1 | 4.0 | 5.0 | 4.0 | 4.0 | 3.0 | 2.0 | 4.0 | 1.0 | 0.0 | 5.0 | 2.0 | 3.0 | 2.0 | 6.0 | 4.0 | 3.0 | 7.0 | 8.0 | 8.0 | 7.0 | 6.0 | 4.0 | 4.0 | 5.0 | 2.0 |
| 2 | 3.0 | 3.0 | 3.0 | 1.0 | 1.0 | 0.0 | 1.0 | 0.0 | 0.0 | 1.0 | 0.0 | 1.0 | 0.0 | 3.0 | 2.0 | 2.0 | 6.0 | 5.0 | 6.0 | 5.0 | 4.0 | 2.0 | 3.0 | 3.0 | 2.0 |
| 3 | 2.0 | 2.0 | 1.0 | 1.0 | 1.0 | 1.0 | 1.0 | 0.0 | 2.0 | 1.0 | 1.0 | 1.0 | 2.0 | 3.0 | 2.0 | 3.0 | 6.0 | 7.0 | 5.0 | 4.0 | 3.0 | 2.0 | 2.0 | 2.0 | 2.0 |
| 4 | 3.0 | 3.0 | 4.0 | 3.0 | 4.0 | 3.0 | 3.0 | 2.0 | 2.0 | 4.0 | 3.0 | 3.0 | 2.0 | 7.0 | 5.0 | 4.0 | 8.0 | 7.0 | 7.0 | 6.0 | 6.0 | 5.0 | 5.0 | 5.0 | 2.0 |
| 5 | 4.0 | 3.0 | 2.0 | 3.0 | 3.0 | 2.0 | 4.0 | 2.0 | 3.0 | 5.0 | 3.0 | 2.0 | 3.0 | 6.0 | 4.0 | 4.0 | 8.0 | 7.0 | 8.0 | 6.0 | 5.0 | 4.0 | 4.0 | 3.0 | 2.0 |
| 6 | 4.0 | 5.0 | 4.0 | 4.0 | 3.0 | 2.0 | 3.0 | 2.0 | 2.0 | 3.0 | 3.0 | 4.0 | 2.0 | 7.0 | 6.0 | 5.0 | 7.0 | 8.0 | 8.0 | 9.0 | 7.0 | 6.0 | 5.0 | 5.0 | 3.0 |
| 7 | 6.0 | 6.0 | 5.0 | 5.0 | 4.0 | 4.0 | 4.0 | 3.0 | 5.0 | 6.0 | 5.0 | 4.0 | 5.0 | 8.0 | 6.0 | 5.0 | 8.0 | 8.0 | 8.0 | 8.0 | 7.0 | 7.0 | 7.0 | 7.0 | 3.0 |
| 8 | 3.0 | 4.0 | 3.0 | 2.0 | 2.0 | 2.0 | 3.0 | 1.0 | 1.0 | 3.0 | 1.0 | 1.0 | 2.0 | 5.0 | 4.0 | 2.0 | 8.0 | 8.0 | 7.0 | 8.0 | 5.0 | 6.0 | 4.0 | 5.0 | 2.0 |
| 9 | 4.0 | 3.0 | 2.0 | 3.0 | 2.0 | 2.0 | 4.0 | 2.0 | 1.0 | 2.0 | 2.0 | 3.0 | 0.0 | 4.0 | 5.0 | 3.0 | 9.0 | 8.0 | 8.0 | 7.0 | 6.0 | 5.0 | 4.0 | 3.0 | 3.0 |
| 10 | 4.0 | 2.0 | 2.0 | 2.0 | 1.0 | 1.0 | 2.0 | 0.0 | 2.0 | 4.0 | 4.0 | 2.0 | 4.0 | 4.0 | 3.0 | 4.0 | 8.0 | 7.0 | 8.0 | 7.0 | 5.0 | 4.0 | 4.0 | 3.0 | 2.0 |
| MEAN | 3.7 | 3.6 | 3.0 | 2.8 | 2.4 | 1.9 | 2.9 | 1.3 | 1.8 | 3.4 | 2.4 | 2.4 | 2.2 | 5.3 | 4.1 | 3.5 | 7.5 | 7.3 | 7.3 | 6.7 | 5.4 | 4.5 | 4.2 | 4.1 | 2.3 |
| STD | 1.0 | 1.2 | 1.1 | 1.2 | 1.1 | 1.0 | 1.1 | 1.0 | 1.3 | 1.5 | 1.4 | 1.1 | 1.4 | 1.6 | 1.3 | 1.0 | 0.9 | 0.9 | 1.0 | 1.4 | 1.1 | 1.5 | 1.2 | 1.4 | 0.4 |

Figure 7: Processed image having α = 0.5 and λ = 0.5

If we compare the processed and original image, this can be noticed that the processed images provide more information to the viewer. In original image no information was there in the dark regions but the processed image refines the information provided in the dark areas.

Table 2 shows the measured quality and standard deviation of 24 randomly selected images after considering the mean opinion score (MOS) from ten subjects for each image. The mean opinion score (MOS) given by the ten subjects/people is shown in Table 3. Each subject rated the processed and unprocessed images as per his opinion and perception. The marks were given out of 10 for each digital image. The results shows that the subjects were not able to distinguish between the processed and the unprocessed or original image.

Figure 8: Processed image having α = 0.05 and λ = 0.45

All the subjects rated the original image as poor. The average score given to it by ten subjects were 2.3. The images which were given highest score of all 25 images were 17 to 20. These images were having α=-0.1,0.5,-0.2,0.25 respectively and λ=1 for all the images. The

image 18 having λ=1 and α=0.5 got the highest average score of all the randomly selected 24 images.

## 4. CONCLUSION

This technique is suited for dark images while for daylight images, it gets deteriorated. The original dark image provides lesser information but after processing same image provides a lot of information, though quality of color deteriorates a little. The processed images appear as if they were taken in the daylight. The results of MOS show that on the average no one was able to distinguish between the original and processed image. Every subject rated the processed image as the better one. Hence, in this paper we analyzed the results using particular technique to enhance the quality of natural dark images.

Our future work is applying the same technique on the medical scans, i.e., on ultrasound or MRI images and evaluate out experimentally, whether this technique refines the results for medical science or not.

## REFERENCES

[1]. R. Gonzalez. R. Woods. "Digital Image Processing," 2nd edition, Prentice Hall, 2002

[2]. S. Rajput, S.R.Suralkar, "Comparative Study of Image Enhancement Techniques," IJCSMC, Vol. 2, Issue. 1, 2013.

[3]. H. R. Tizhoosh, B. Michaelis, "Subjectivity, psychology and fuzzy techniques: a new approach to image enhancement," in Proc. 18th International Conference of the North American, pp.522-526, 1999.

[4]. R. Maini and H. Aggarwal, "A Comprehensive Review of Image Enhancement Techniques," Journal of Computing, Vol. 2, Issue 3, pp.8-13, 2010,.

[5]. G. Woodell, D. J. Jobson, Z. Rahman, and G.A Woodell, "Properties and performance of a center/surround Retinex," IEEE Transactions in Image processing, Vol. 6, pp.451-462, 1997.

[6]. C. T. Vu, T. D. Phan, P. S. Banga, and D. M. Chandler, "On the quality assessment of enhanced images: A database, analysis, and strategies for augmenting existing methods," IEEE Symposium on Image Analysis and Interpretation, pp. 181–184, 2012.

[7]. P. R. Naoum, "Color Image Enhancement Using Steady State Genetic Algorithm," WCSIT, vol. 2, no. 6, pp. 184–192, 2012.

[8]. N. S. Bagri, "Images Enhancement with Brightness Preserving using MRHRBFN," International Journal of Computer Applications, Vol. 40, no. 7, pp. 22–26, 2012.

[9]. S. Arya and P. Lehana, "Development of seed analyzer using the techniques of computer vision," International Journal of Distributed and Parallel Systems, Vol.3, no.1, pp. 149-155, 2012.

[10]. P. Lehana, S. Devi, S. Singh, P. Abrol, S. Khan, S. Arya, "Investigations of the MRI Images using Aura Transformation," Signal & Image Processing: An International Journal, Vol.3, no.1, pp. 95-104, 2012.

[11]. Y. Chen, Y. Ho, C. Wu, C. Lai, "Arial Image Clustering using genetic Algorithim," International conference on Computational Intelligence for measurement systems and applications, pp. 42-45, 2009.

[12]. M. F. Al, "A New Enhancement Approach for Enhancing Image of Digital Cameras by Changing the Contrast," International Journal of Advanced Science and Technology, Vol. 32, pp.13-22, 2011.

[13]. Priti Rajput, Santoresh Kumari, Sandeep Arya, Parveen Lehana, "Effect of Diurnal Changes on the Quality of Digital Images," Physical Review & Research International, vol. 3, no. 4, pp. 556-567, 2013.

[14]. Glenn Woodell, Daniel. J. Jobson, Zia-ur Rahman, and Glenn Hines, "Enhanced images for checked and carry-on baggage and cargo screening," In Proc. SPIE Sensors, and Command, Control, Communications, and Intelligence (C3I) Technologies for Homeland Security and Homeland Defense III, pp. 5403, 2004.

[15]. T. A. Mahmood, "Enhancement of Arial Images using Threshold Decomposition Adaptive Morphological Filter," 16TH IEEE International Conference on Image processing, pp. 3121-3124, 2009.

[16]. K. K. Lavania, Shivali, R. Kumar, "Image Enhancement using Filtering Techniques," International Journal on Computer Science and Engineering, Vol. 4, No. 01, 2012.

[17]. A. Goyal, A. Bijalwan, P. Kumar, and K. Chowdhury, "Image Enhancement using Guided Image Filter Technique," IJEAT, Vol. 1, no. 5, pp. 213–217, 2012.

[18]. K. R. Hole, P. V. S. Gulhane, and P. N. D. Shellokar, "Application of Genetic Algorithm for Image Enhancement and Segmentation," IJARCET, vol. 2, no. 4, pp. 1342–1346, 2013.

[19]. M. F. Al-Samaraie, "A New Enhancement Approach for Enhancing Image of Digital Cameras by Changing the Contrast," International Journal of Advance Science and Technology, vol. 32, pp. 13–22, 2011.

[20]. S. O. Mundhada, "Image Enhancement and Its Various Techniques," International Journal of Advanced Research, vol. 2, no. 4, pp. 370–372, 2012.

[21]. G. Gilboa, N. Sochen, and Y. Y. Zeevi, "Image enhancement and denoising by complex diffusion processes," IEEE Transactions on Pattern Analysis and Machine Intelligence, vol. 26, no. 8, pp. 1020–36, 2004.

[22]. R. Chanana, E. Parneet, K. Randhawa, E. Navneet, and S. Randhawa, "Spatial Domain based Image Enhancement Techniques for Scanned Electron Microscope (SEM) images," IJCSI, vol. 8, no. 4, pp. 580–586, 2011.

[23]. S. Arya, S. Khan, D. Kumar, M. Dutta, P. Lehana, "Image enhancement technique on Ultrasound Images using Aura Transformation," International Journal in Foundations of Computer Science & Technology, Vol.2, no.3, pp. 1-10, 2012.

[24]. "Digital Image Processing for Image Enhancement and Information Extraction," http://civil.iisc.ernet.in/~nagesh/rs_docs /Imagef.pdf

 

[25]. A. V. Deorankar, P. N. Chatur, R. S. Mawale, "Journal of Computing::Photo Vista Image Processing Tool," vol. 3, no. 10, pp. 1368–1372, 2012.

[26]. F. Mu. Abubakar, "Image Enhancement using Histogram Equalization and Spatial Filtering," International Journal of Science and Research (IJSR), Vol. 1 Issue 3, 2012.

[27]. S. O. Mundhada, V. K. Shandilya, "Spatial and Transformation Domain Techniques for Image Enhancement," IJESIT, Vol.1, Issue 2, 2012.

[28]. P. Jain, G. Kaur, "Analysis the Impact of Filters in Spatial Domain on Grayscale Image," International Journal of Computer Applications, Vol. 36, no.7, 2011.

[29]. M. A. A. Moustaf,. H. M. Ismaiel, "Quantitative and qualitative evaluations of image enhancement techniques,", 46th IEEE Midwest Symposium on Circuits and Systems, Vol.2, pp.664-669, 2003.

[30]. P. Nithyanandam, T. Ravichandran, N. M. Santron and E. Priyadarshini, "A Spatial Domain Image Steganography Technique Based on Matrix Embedding and Huffman Encoding," IJCSS, Vol. 5, Issue 5, 2011.

[31]. A. O. Karali, T. Aytac, "A comparison of different infrared image enhancement techniques for sea surface targets," 17th IEEE Conference on Signal Processing and Communications Applications, pp.765-768, 2009.

[32]. H. H. Cho; S. H. Kim, T. K. Cho, M. R. Choi, "Efficient image enhancement technique by decimation method," IEEE Transactions on Consumer Electronics, Vol.51, no.2, pp.654-659, 2005.

[33]. Dwitej, O. Sudhakar, V. Sailaja, "Traditional Color video Enhancement Based On Adaptive Filter," IJERT, Vol. 1, no. 9, pp. 1–4, 2012.

[34]. S. Erkanli, Z. Rahman, "Enhancement Technique for Uniformly and Non-Uniformly Illuminated Dark Images," 10th International Conference on Intelligent Systems Design and Applications), pp. 850-854, 2010.

[35]. S. Erkanli, Z. Rahman, "Wavelet Based Enhancement Technique for Uniformly and Non-Uniformly Illuminated Dark Images," 10th International Conference on Intelligent Systems Design and Applications), pp. 855-859, 2010.

[36]. S. Erkanli, J. Li and E. Oguslu, "Fusion of Visual and Thermal Images using Genetic Algorithms," Bio Inspired Computational Algorithims and their Applications, pp. 187-212, www.intenchopen.com.